DOI: 10.21062/mft.2024.019 http://www.journalmt.com

The Effect of Laser Welding Parameters on Aluminium PV Construction Rack Systems

Pavel Houška (0000-0003-4295-258X)[1], Klára Caisová (0000-0001-6708-6214)[2] , Vladislav Síťař (0000-0002-6476-8153)[1], Štefan Michna (0000-0001-5893-5050)[1], Tomáš Alfonso (0009-0001-9474-9551)[2]
[1]Faculty of Social and Economic Studies, J. E. Purkyne University in Usti nad Labem. Moskevska 54, 400 96 Usti nad Labem. Czech Republic. E-mail: pavel.houska@ujep.cz
[2]Faculty of Mechanical Engineering, J. E. Purkyne University in Usti nad Labem. Pasteurova 3334/7, 400 01 Usti nad Labem. Czech Republic. E-mail: klara.caisova@ujep.cz

Rising energy demands together with environmental concerns have spurred increased focus on renewable energetics, leading to the widespread installation of photovoltaic power plants worldwide. Due to the unique solar dispersion angle over the world, different racking systems are also the subject of keen interest in mechanical support equipment. Different constructions require welded joints of construction parts with massive strain while exposed to weather conditions. Therefore mechanical properties of the joints of these systems are being also studied. This research is focused on the mechanical properties (such as microstructure and microhardness) of aluminium laser welded joints under different welding parameters. The main aim of this paper is to find ideal parameters of laser welded aluminium profiles ensuring durable construction for PV panels.

Keywords: Aluminium, Laser welding, Solar panels, Racking system construction, Microstructure

1 Introduction

The main motivation of this research is to find an adequate alternative for assembled structures widely used for photovoltaic (PV) rack systems. By using welded joints, the construction can acquire lower mass, higher corrosion resistance [1] and better recyclability [2].

Solar energy, harnessed through photovoltaic (PV) systems, holds immense promise as a clean and sustainable energy source [3]. Terrestrial solar energy amounts to around 1.8 × 1011 MW every year, which is around 10,000 times the rate of the global energy demand [4]. Increasing consumption of electrical energy from primary energy resources increases CO_2 emissions, which has a great impact on the environment [5,6,7]. Therefore, there is an eminent interest on the part of engineers and scientists with a focus on the tangible measure of energy savings in maximizing the use of renewable energy sources.

The efficiency of converting solar energy into electrical energy depends essentially on the PV panels that produce electrical power [8]. Currently, the power energy efficiency of the PV panels for commercial engineering applications is within the range of 12–23% (for multi- or mono-crystalline modules, respectively) measured at the Standard Test Conditions (STC) of 1.0 $kW.m^{-2}$, ambient temperature of 25 °C, and wind speed of 1.5 $m.sec^{-1}$ [9].

Much of the cost of a solar system is associated with the supporting materials and frames. For example, approximately 25-30% of the CSP plant budget should be allocated to frames and support materials [10].

Since the tilt of solar panels is known for its major effect of PV panels performance, the construction as a holding mechanism requires different tilt for different locations with different conditions [11].

Therefore the constructions require precise welding for structural integrity [12], and laser welding can be considered as a potential solution. Welded joints can also contribute to better recyclability of the whole construction instead of assembled ones, where steel fasteners can contaminate recycled batches by redundant Fe content [12].

The aluminium construction of the racking system is nowadays also subjected to examination for its passive cooling ability [13].

Approximately 72% of the aluminium input in PV solar systems is used in construction, while the proportion of aluminium used in panel frames and inverters is 22% and 6%, respectively [14].

Aluminium construction racks, integral to PV installations are nowadays being subjected to research from different points of view [15]. Aluminium alloy 6061, which contains the alloying elements magnesium and silicon, is an example of a useful aluminium alloy for solar power plant construction. This aluminium alloy is widely used in solar arrays because of its high strength [16] and machinability [17, 18].

ISSN 1213–2489
e-ISSN 2787–9402

2 Materials and methods

This research is focused on a rack system holding PV panels installed on the roof of a multifunction building located in Ústí nad Labem (see Fig. 1). Samples were cut out of welded construction profiles made from Aluminium alloy 6061. The welding output ranges from 75 to 95 %. These samples were labelled as 1 - 4 according to the used output. Samples were subsequently cross-sectioned and subjected to further analysis.

Fig. 1 *Rack system holding PV panels of the given location*

In order to investigate laser welding parameters to enhance PV system durability and efficiency, aluminium profiles were welded under different conditions. Four samples of laser welds were subjected to investigate the effect of percentage outputs. Labelled samples are reported in Tab. 1.

Tab. 1 *Output percentage used for welding the aluminium profiles*

Sample	1	2	3	4
Percentage of Output	75	80	85	95
Welding Performance [W]	1125	1200	1275	1425

3 Welding technology

The manual laser welding technique was employed to create welds on aluminium profiles with a square cross-section (40 x 40 mm outer dimension, 4 mm wall thickness), utilizing the LaserTherm handheld welding machine with maximal output from 1 500 W. Prior to welding, the profiles were cut at a 45° angle using a circular saw and secured in the desired position using a jig for subsequent welding. Following the formation and cooling of the weld in ambient air, the weld surface underwent machining (alignment) using a disc grinder. The resulting machined weld is depicted in Figure 2.

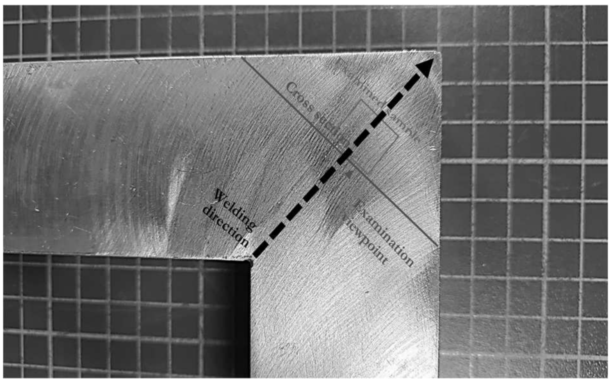

Fig. 2 *Welded profile*

The chemical composition analysis of the profile was conducted utilizing a Q4 TASMAN optical emission spectrometer. Table 2 showcases the results of average values for 3 measurements obtained from this analysis.

***Tab. 2** Chemical composition of the analysed alloy [wt. %]*

Chemical composition	average
Mg	0.473
Al	98.713
Si	0.583
Mn	0.033
Fe	0.180
Zn	0.010

The chemical composition analysis revealed the identified aluminium alloy to be EN AW 6060 (AlMgSi0.5). Table 3 outlines the chemical composition of this alloy as specified by EN 573-4.

***Tab. 3** Chemical composition of alloy EN AW 6060 (AlMgSi0.5) according to EN 573-4*

Al	97.9 – 99.3
Cr	max 0.05
Cu	max 0.1
Fe	0.1-0.3
Mg	0.35-0.50
Mn	max. 0.1
Si	0.3-0.6
Ti	max 0.1
Zn	max 0.15
Other	max 0.15

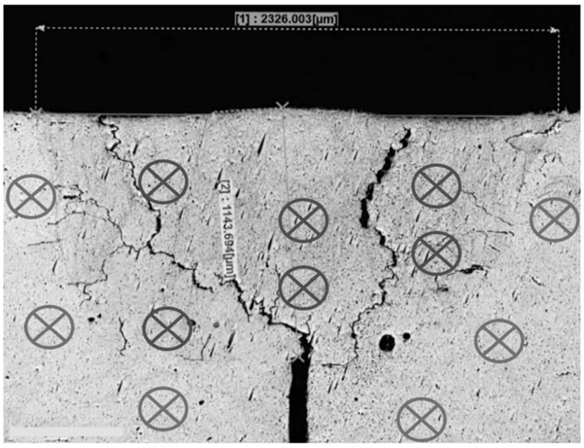

Cross section of sample 1

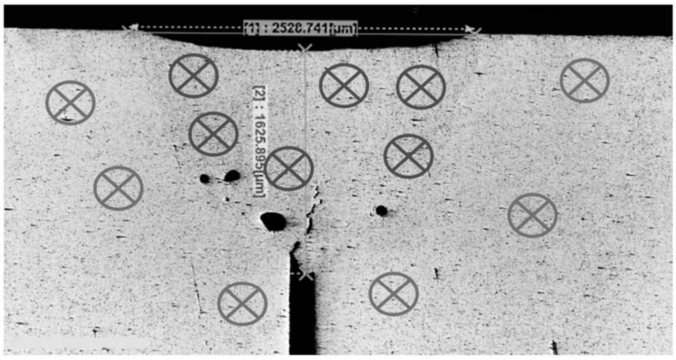

Cross section of sample 2

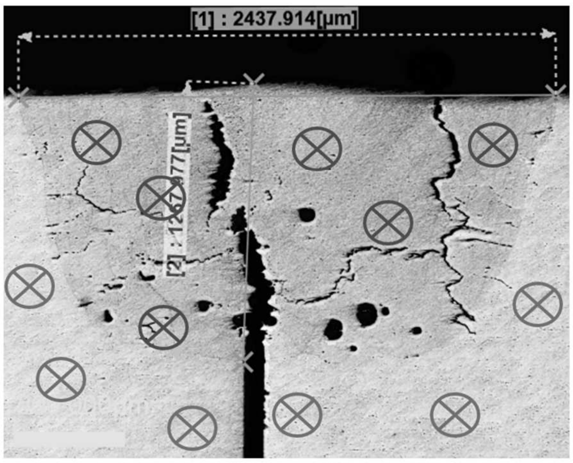

Cross section of sample 3

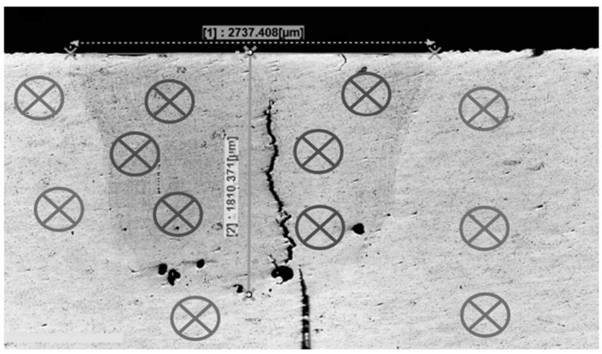

Cross section of sample 4

***Fig. 3** Microstructure analysis of analysed samples with marked positions of the microhardness measurements*

Microhardness measurements were conducted on metallographic samples taken from a perpendicular section of the welded joint. The actual measurements were performed using a Shimadzu HMV-2 microhardness tester applying a load of 25 grams for a duration of 10 seconds.

The assessment of microhardness for the base material, specifically the EN AW 6060 alloy, involved conducting measurements on a section of the profile situated entirely distanced from the weld joint (red marks) and its corresponding heat-affected zone (green marks). Within this evaluation of the base material's microhardness, 9 random measurements were systematically taken across all analyzed samples. The documented microhardness values of the base material are presented in Table 4.

During the microhardness analysis of each specimen's welds, measurements were taken along the weld axis and within the heat-affected zone (HAZ), specifically at the interface between the weld and the base material. These measurements were consistently obtained 2 mm away from the weld axis for each specimen. The microhardness measurement outcomes for both the weld and the heat-affected zone of each specimen are detailed in Table 5.

Tab. 4 *Results of microhardness measurements of the base material*

Measurement number	**HV0.025**
1	95.9
2	97.0
3	98.5
4	99.4
5	100.0
6	99.4
7	95.3
8	93.3
9	95.9
Average	97.2
Standard deviation	2.146

Tab. 5 *Results of microhardness measurements of samples in the weld and heat-affected zone (HAZ)*

Sample	**Sample 1**		**Sample 2**		**Sample 3**		**Sample 4**	
Measurement number	Weld	HAZ	Weld	HAZ	Weld	HAZ	Weld	HAZ
1	56.70	59.80	54.00	65.00	52.70	57.30	48.70	58.70
2	55.70	59.90	51.20	68.40	55.30	57.30	49.20	61.00
3	50.60	57.60	49.90	70.60	56.10	56.40	46.10	60.70
4	49.80	60.00	48.90	62.80	56.30	55.50	48.60	59.90
5	49.50	58.10	50.40	72.60	57.10	57.90	48.30	58.20
6	48.00	59.40	52.00	66.70	57.40	58.10	45.80	59.70
Average	**51.71**	**59.13**	**51.07**	**67.69**	**55.81**	**57.09**	**47.78**	**59.70**
Standard deviation	3.28	0.94	1.63	3.30	1.55	0.89	1.33	1.00

4 Results and Discussion

The chemical composition analysis confirmed that the welded profiles matched the chemical composition standards of the EN AW 6060 alloy, as outlined in EN 573-4. All identified elements concentrations fell within the specified range set by the standard.

The microstructure analysis revealed distinct characteristics in the perpendicular section of each sample's weld, directly linked to the welding power applied. Beyond differences in the weld sizes (with depths ranging approximately from 1200 to 1800 μm and widths around 2300 to 2700 μm), numerous internal flaws were observed within the welded joints. Circular pores were uniformly present in all analyzed welds, notably concentrated at the base of the weld. The identified porosity, exhibited in a circular morphology, is attributed to the diffusion of protective gases into the molten weld pool during the welding process.

Additionally, individual welds exhibited cracks (caused by the intercrystalline stress due to the rapid solidification during the welding process), the extent of which was notably influenced by the welding power utilized. Notably, specimen 3 demonstrated the highest occurrence of internal defects, both cracks and pores, at the interface between the weld and the heat-affected zone. Conversely, sample 2 exhibited the lowest incidence of both pores and cracks within the weld and at the interface between the weld and the heat-affected zone.

The microhardness assessment of the base material (EN AW 6060 alloy profiles) displayed consistent solid solution microhardness, averaging 97.2 HV0.025 across all analyzed samples. However, the microhardness within the weld joint along the weld axis varied, ranging between 47.8 to 55.8 HV0.025 across the samples. In the heat-affected zone, measured at a distance of 2 mm from the weld axis, the microhardness spanned from 57.1 to 67.7 HV0.025.

Notably, specimen 2 exhibited the smallest disparity in microhardness between the heat-affected zone and the base material among all samples.

Samples were cross-sectioned and subsequently examined via Laser confocal microscope OLYMPUS LEXT OLS 5000. Figure 3 shows the cross-section of analysed samples.

5 Conclusion

Based on the conducted analyses, several conclusions can be drawn:

- Laser welding performance significantly impacts weld quality, particularly the presence of internal flaws like pores and cracks.
- Welding performance is intricately linked to residual stresses in both the weld area and the heat-affected zone, evident through varying microhardness values within these regions.
- Optimal outcomes, considering both internal defect occurrence in the weld and the smooth transition of microhardness between the weld, heat-affected zone, and base material, seem to align with the application of laser welding at a power level of 1 200 W (sample labelled as 2).
- Based on the results of the analyses, the technology of manual laser welding of aluminium profiles (while observing the optimal welding parameters) appears to be a usable substitute for the technology of assembled constructures for photovoltaic panels.

Acknowledgement

This research was supported via SGS grant number 45208/15/2009/01 within the student grant competition at UJEP and OP VVV Project Development of new nano and micro coatings on the surface of selected metallic materials - NANOTECH ITI II., Reg. No CZ.02.1.01/0.0/0.0/18_069/0010045.

References

[1] KOVALČÍK, T., STOULIL, J., SLAMA, P., VOJTĚCH, D. (2015). The Influence of Heat Treatment on Mechanical and Corrosion Properties of Wrought Aluminium Alloys 2024 and 6064. *Manufacturing Technology*. 15. 54-61. 10.21062/ujep/x.2015/a/1213-2489/MT/15/2/148.

[2] ABE, N., MORIKAWA, A., TSUKAMOTO, M., MAEDA, K., NAMBA, K. (2003). Welding of aluminium alloy with high power direct diode laser. *Proceedings* of SPIE - The International Society for Optical Engineering. 10.1117/12.478376.

[3] VICTORIA, M., HAEGEL, N., PETERS, I. M., SINTON, R., JÄGER-WALDAU, A., CAÑ, C., BREYER, C., STOCKS, M., BLAKERS, A., KAIZUKA, I., KOMOTO, K., SMETS, A. (2021). Solar photovoltaics is ready to power a sustainable future. *Joule*. 5. 10.1016/j.joule.2021.03.005.

[4] SIECKER, J., KUSAKANA, K., NUMBI, B. P. (2017). A review of solar photovoltaic systems cooling technologies. *Renew. Sustain. Energy Rev*, 79, 192–203.

[5] LI, X., WU, W., YU, C. W. F. (2015) Energy demand for hot water supply for indoor environments: Problems and perspectives. *Indoor Built Environ.* 24, 5–10.

[6] CHAKAMERA, C., ALAGIDEDE, P. (2018) Electricity crisis and the effect of CO2 emissions on infrastructure-growth nexus in Sub Saharan Africa. *Renew. Sustain. Energy Rev*, 94, 945–958.

[7] YOUSEF, B. A. A., HACHICHA, A. A., RODRIGUEZ, I., ABDELKAREEM, M.A., INYAAT, A. (2007) Perspective on integration of concentrated solar power plants. *Int. J. Low-Carbon Technol.* 2021, 1–28.

[8] CHOW, T. T., JI, J., HE, W. (2007) Photovoltaic-Thermal Collector System for Domestic Application. *J. Sol. Energy Eng.* 129, 205–209.

[9] MAKKI, A., OMER, S., SABIR, H. (2015) Advancements in hybrid photovoltaic systems for enhanced solar cells performance. *Renew. Sustain. Energy Rev.* 41, 658–684.

[10] FARZANEH, A., MOHAMMDI, M., AHMAD, Z., AHMAD, I. (2012) *Aluminium Alloys in Solar Power – Benefits and Limitations.* DOI: 10.5772/54721,

[11] BARBÓN, A., FORTUNY-AYUSO, P. O., BAYÓN, L., SILVA, C. A. (2021). A comparative study between racking systems for photovoltaic power systems. *Renewable Energy*. 180. 10.1016/j.renene.2021.08.065.

[12] SAHUL, M., TURŇA, M., ŠUGÁROVÁ, J., SAHUL, M. (2013). Influence of Laser Welding Aluminium Alloy on Mechanical Properties of Welded Joints. *Manufacturing Technology*. 13. 526-530. 10.21062/ujep/x.2013/a/1213-2489/MT/13/4/526.

[13] AL-AMRI, F., SAEED, F., MUJEEBU, M. A. (2022). Novel dual-function racking structure for passive cooling of solar PV panels –thermal performance analysis. *Renewable Energy*. 198. 10.1016/j.renene.2022.08.047.

[14] BÖDEKER, J. M., BAUER, M., PEHNT, M. (2010). Aluminium and Renewable Energy Systems – prospects for the Sustainable Generation of Electricity and Heat. 2010 Resources, America's & Sciences, National & Engineering, National & Council, National. *Electricity from renewable resources: Status, prospects, and impediments*. 10.17226/12619.

[15] RADU, A., AXINTE, E., THEOHARI, C. (1986). Steady wind pressures on solar collectors on flat-roofed buildings. *Journal of Wind Engineering and Industrial Aerodynamics* - J WIND ENG IND AERODYN. 23. 249-258. 10.1016/0167-6105(86)90046-2.

[16] CHOCHLÍKOVÁ, H., MAJERNÍK, J., BARÉNYI, I., ESCHEROVÁ, J., PECANEC, M., RAJNOVIC, D., BALOŠ, S., KOHUTIAR, M. (2024). Research on FSW Welds of Al-Alloy Modified by Laser Shock Peening Process. *Manufacturing technology*. 10.21062/mft.2024.018.

[17] TJOTTA, S. Advantages o extruded aluminium in solar power generation systems processes. A*dvanced Materials and Processes* 2011;169(1): 28-9.

[18] BRADÁČ, J., SOBOTKA J. (2023). Evaluation of Riveting Force Influence on the Quality of Riveted Joint of Aluminium Alloy EN AW - 6016. *Manufacturing Technology*. 23. 10.21062/mft.2023.011.